Time-Shift Technique for Characterization of Transparent Particles in Sprays

Walter Schäfer[1,*], Cameron Tropea[1,2]

1: Institute of Fluid Mechanics and Aerodynamics, Technische Universität Darmstadt, Germany
2: Center of Smart Interface, Technische Universität Darmstadt, Germany
* Corresponding author: w.schaefer@sla.tu-darmstadt.de

Abstract A novel implementation of the time-shift technique for particle/droplet sizing is introduced which uses two time-shift signals to determine refractive index and uses the signal peak width to estimate velocity. The particle size is determined directly from the time-shift between signals arising from the reflection and second-order refraction scattering orders. The system presented here utilizes a laser diode as a light source and is configured to operate in near backscatter; hence, a compact, relatively inexpensive and robust system for particle size, refractive index and velocity is presented.

1. Introduction

Particle, and in particular droplet sizing is of prime importance when characterizing sprays and other atomization processes. A multitude of techniques exist for determining size, including phase Doppler, ILIDS/IPI, Mie/LIF and techniques based on femtosecond illuminating pulses: a review of available techniques is available in Tropea (2011) [1]. Velocity is usually determined by combining the sizing technique with a laser Doppler or time-of-flight technique [2]. Very few techniques are available for determining refractive index of individual droplets in-situ, for example rainbow refractometry [3]. Furthermore, most existing techniques for size measurements require *a priori* knowledge about the refractive index. Therefore, a need exists for a technique measuring size, velocity and refractive index in a single instrument, preferably for individual droplets and preferably in a near-backscatter configuration, for case in which perhaps only one optical access to the measurement position is available. The development of such a technique was exactly the goal of the present work. Although the time-shift technique is a known measurement method, until now it has not been applied to spray characterization because of several secondary problems. These problems will be outlined and several enhancements will be introduced, making the technique much more attractive and reliable for spray characterization. In particular validation criteria have been found which greatly improve the reliability of individual drop measurements.

2. Measurement Principle

The time-shift technique is used here in a somewhat modified form. This technique was first introduced by Semidetnov (1985) [4] and was further developed in Damaschke et al (2002) and Albrecht et al (2003)[5]. The time-shift technique has also been called the pulse displacement technique and several variations have been discussed by Hess and Wood (1993)[6] and Lin et al. (2000)[7]. The technique requires an illuminated volume considerably smaller than the size of the particle to be measured, usually taking a Gaussian beam shape in intensity. Under these conditions the scattering from a spherical droplet can be interpreted according to various scattering orders, well described by employing a Debye series [8] expansion of the Mie [9] scattering functions or using a geometric optics [10] approach to compute the scattering field. Effectively a different measurement volume is realized for each scattering order, and each measurement volume is displaced in space from one another (Figure 1). The magnitude of this displacement depends on the particle size, velocity, refractive index and the scattering angle. When the particle passes through these different measurement volumes, the measurement volume displacement appears as a time shift of the signal on any one single detector.

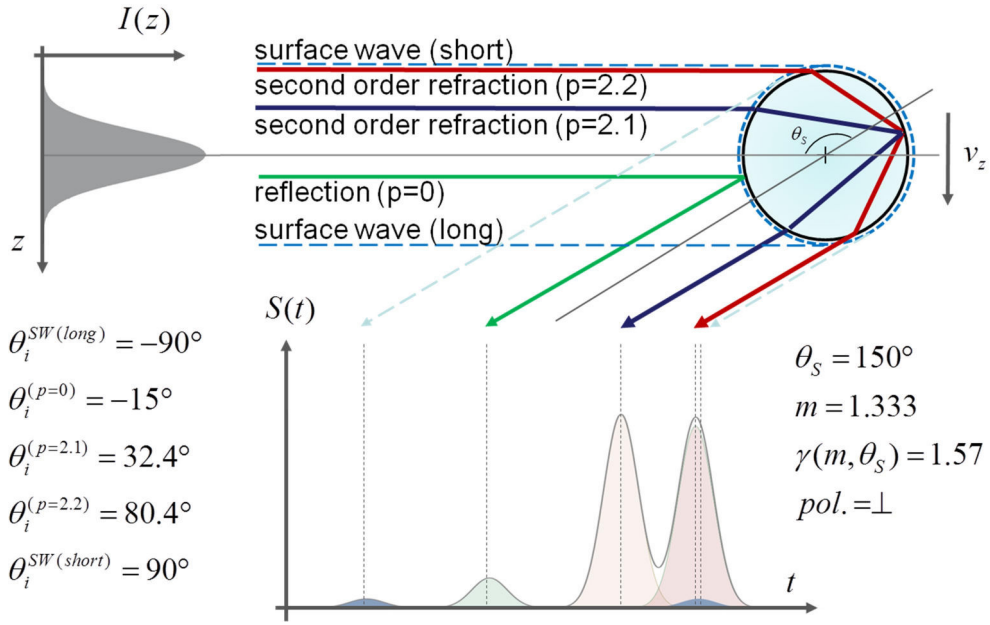

Figure 1: Basic principle of time-shift technique.

Depending on scattering angle and relative refractive index there are different scattering orders with their respective incident points and glare points, which can be calculated by ray tracing methods. When a particle with velocity v and size d passes through a shaped beam, typically Gaussian in intensity, it transforms the intensity of light beam in space $I(x)$ into a time signal $S(t)$, being the sum of all scattering orders (reflection (p=0) and second-order refraction (p=2) for backscatter) and their respective modes (p=2.1 and p=2.2). The time dependent signal can then be expressed in the form:

$$I(x) = I_0 \exp\left(-\frac{2(x-x_0)^2}{w_0^2}\right) \xrightarrow{x=vt}$$
$$I_0 \exp\left(-\frac{2v^2(t-t_0)^2}{w_0^2}\right) = \sum_{\substack{p=0\\p=2.1\\p=2.2}} A_p \exp\left(-\frac{2\left(t-t_0^{(p)}\right)^2}{\sigma^2}\right) = S(t) \qquad (1)$$

where w_0 is the size of illumination beam at the beam waist, A_p the amplitudes and $t_0^{(p)}$ the time position of the scattering orders. The time width of individual peaks in a time-shift signal is characterized by σ, which is given by

$$\sigma = \frac{w_0}{v} \qquad (2)$$

According to Eq. (2) the width of individual peaks is inversely proportional to the particle velocity, so that the particle velocity can be calculated by knowing the size of the illuminating beam and measuring the width of the peaks in the signal. The shape of each individual peak (reflection, second-order refraction) takes the shape (and width) of the illuminating beam intensity profile.
The experimental setup presented here consists of two photo-detectors placed symmetrically around the light source at a scattering angle about 160deg (Figure 2). The collimated laser beam is focused by a single cylindrical lens to a sheet with thickness of approx. 38µm and approx. width of 1000µm.

The thickness of the laser sheet should be smaller than the droplet size in order to obtain the characteristic time-shift signal (Figure 3). If the laser sheet thickness is in the range or larger than the droplet/particle size, the time-shift signal is not suitable because the signal peaks from different scattering orders overlap too much to be uniquely distinguished.

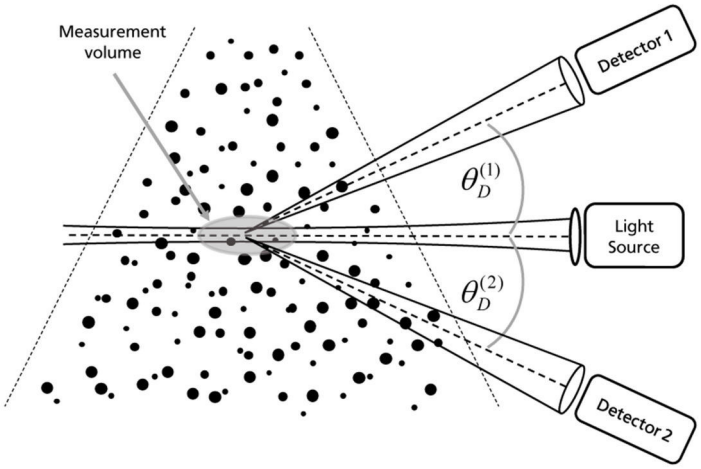

Figure 2: Schematic illustration of the experimental setup.

The signal for a scattering angle in backscatter coming from one droplet is composed of several peaks, corresponding to scattering by reflection (p=0) and two modes of second-order refraction (p=2.1, p=2.2). The interference between scattering orders does not occur, because they are temporally separated. Although the signal from one photo-detector is sufficient to calculate the particle size and velocity, the signal from the second photo-detector provides redundant information and is used to increase the accuracy of the measurement; moreover the measurement volume can be more precisely defined spatially.

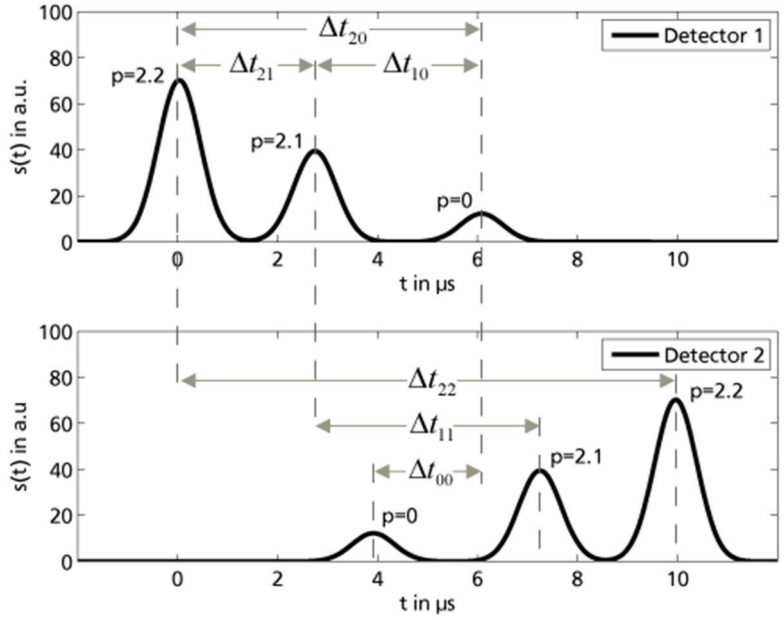

Figure 3: The characteristic time-shift signals for both detectors for refractive index 1.34, scattering angle 155deg, velocity 10m/s, particle size 100µm and the beam size 15µm.

The signals coming simultaneously from the two detectors are illustrated in Figure 3. The time durations between peaks are characteristic for a given relative refractive index and scattering angle, taking into account the velocity and the size of a particle. If the velocity is calculated from the width of individual peaks using equation (2), the particle size can be determined from the time duration between peaks, knowing beforehand the relative refractive index and scattering angle. According to Figure 3 there are six time durations between peaks in two time-shift signals, although only three of them are linear independent. According to geometrical optics these time differences can be related to the size, velocity and relative refractive index through the following expressions:

$$\Delta t_{10}(d,v,\theta_S,m)=\frac{d/2}{v}\left(\cos\left(\frac{\theta_S}{2}\right)+\sin\left(\theta_i^{(p=2.1)}(\theta_S,m)\right)\right)=\frac{d}{v}f_{10}(\theta_S,m) \tag{3}$$

$$\Delta t_{20}(d,v,\theta_S,m)=\frac{d/2}{v}\left(\cos\left(\frac{\theta_S}{2}\right)+\sin\left(\theta_i^{(p=2.2)}(\theta_S,m)\right)\right)=\frac{d}{v}f_{20}(\theta_S,m) \tag{4}$$

$$\Delta t_{21}(d,v,\theta_S,m)=\frac{d/2}{v}\left(\sin\left(\theta_i^{(p=2.2)}(\theta_S,m)\right)-\sin\left(\theta_i^{(p=2.1)}(\theta_S,m)\right)\right)=\frac{d}{v}f_{21}(\theta_S,m) \tag{5}$$

$$\Delta t_{00}(d,v,\theta_S)=\frac{d}{v}\cos\left(\frac{\theta_S}{2}\right) \tag{6}$$

$$\Delta t_{11}(d,v,\theta_S,m)=\frac{d}{v}\left(\sin\left(\theta_i^{(p=2.1)}(\theta_S,m)\right)\right) \tag{7}$$

$$\Delta t_{22}(d,v,\theta_S,m)=\frac{d}{v}\left(\sin\left(\theta_i^{(p=2.2)}(\theta_S,m)\right)\right) \tag{8}$$

where $\theta_i(\theta_S,m)$ is the incident angle of corresponding scattering order modes as given exemplarily in Figure 1.

3. Instrument Design

The time-shift signal to be processed and validated must have peaks of the reflection (p=0) and two modes of the second-order refraction (p=2.1 and p=2.2). Although reflective scattering exists over the entire scattering angle range, second-order refraction appears only for scattering angles larger than the first rainbow angle and can have one, two or three modes. The number of modes depends on scattering angle and relative refractive index and can be calculated by ray tracing methods. Additionally, at the backscatter angles, third-order refraction occurs for scattering angles lower than the second rainbow angle. If the scattering angle is smaller than this angle, then a peak arising from third-order refraction will occur in the time-shift signal, which is undesirable. Consequently, the scattering angle should be in a range between the first and second rainbow angle and be smaller than the scattering angle, where the third mode or only one mode of second-order refraction exists. This leads to a limitation of the scattering angle and relative refractive indexes as illustrated in Figure 4.

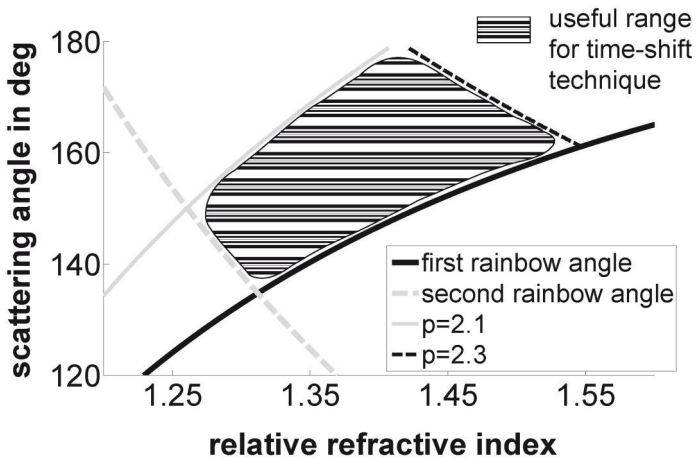

Figure 4: Scattering angle regimes where different scattering orders exist.

In order to analyze the time-shift signal, the individual peaks in the time-shift signal must be recognizable, which demands that the illuminating beam in the measurement volume be of the same size or smaller than the particle to be measured. The ratio between particle size and beam width will be referred to as particle/beam ratio. The particle velocity doesn't influence the separation of individual peaks in the signal, because a higher velocity leads to a reduction of the peak width, but also to a reduction of the time separation, so that the ratio stays constant.
The focused light beams used in experimental setups presented here are Gaussian beams and as a result the individual peaks in a time shift signal can be described by Gaussian functions. In general, for a sufficient resolution of two neighboring Gaussian peaks, their intersection points should be at points of full width at half maximum (FWHM). From this it follows that the necessary conditions for resolving individual peaks in the time-shift signal can be formulated by

$$t_0^{(p=0)} + \frac{FWHM}{2} < t_S^{(p=0,p=2.1)} < t_0^{(p=2.1)} - \frac{FWHM}{2} \tag{9}$$

$$t_0^{(p=2.1)} + \frac{FWHM}{2} < t_S^{(p=2.1,p=2.2)} < t_0^{(p=2.2)} - \frac{FWHM}{2} \tag{10}$$

where t_0 is the time position of peak maxima and t_S is the intersection point between two neighboring Gaussian peaks.
After some mathematical manipulation, these conditions can be reduced to the final two inequalities

$$-\Delta t_{10}^2 + \Delta t_{10} FWHM \pm FWHM^2 \frac{\ln\left(A_{p=0} / A_{p=21}\right)}{4\ln(2)} < 0 \tag{11}$$

$$-\Delta t_{21}^2 + \Delta t_{21} FWHM \pm FWHM^2 \frac{\ln\left(A_{p=21} / A_{p=22}\right)}{4\ln(2)} < 0 \tag{12}$$

where $FWHM$ and Δt can be replaced by equations (2),(3),(5) and the amplitude ratio, being independent of particle size, can be calculated by employing geometrical optics.
After solving equations (11) and (12) the minimal value of the particle/beam ratio, which is necessary for analyzing the time-shift signal, is given by

$$\left(\frac{d_{\min}}{2w_0}\right)^{\substack{p=0\\p=2.1\\p=2.2}} = \max\left(\frac{\sqrt{\ln\left(\sqrt{2}\right)}\left(1+\sqrt{1+\frac{\left|\ln\left(A_{p=0}/A_{p=2.1}\right)\right|}{\ln(2)}}\right)}{\left(\sin\left(\theta_i^{p=0}(\theta_S,m)\right)+\sin\left(\theta_i^{p=2.1}(\theta_S,m)\right)\right)};\frac{\sqrt{\ln\left(\sqrt{2}\right)}\left(1+\sqrt{1+\frac{\left|\ln\left(A_{p=2.1}/A_{p=2.2}\right)\right|}{\ln(2)}}\right)}{\left(\sin\left(\theta_i^{p=2.2}(\theta_S,m)\right)-\sin\left(\theta_i^{p=2.1}(\theta_S,m)\right)\right)}\right) \quad (13)$$

The numerical calculation of (13) is illustrated in Figure 5, where the particle/beam ratio is depicted as a function of scattering angle for different refractive indexes and polarization states. It can be seen that for constant relative refractive index the particle/beam ratio is highly sensitive to the scattering angle as well as to the polarization of the light beam. The minimal possibly achievable particle/beam ratio is about 2.4: for example for a beam width of 10μm the minimal particle size which can be detected is about 24μm.

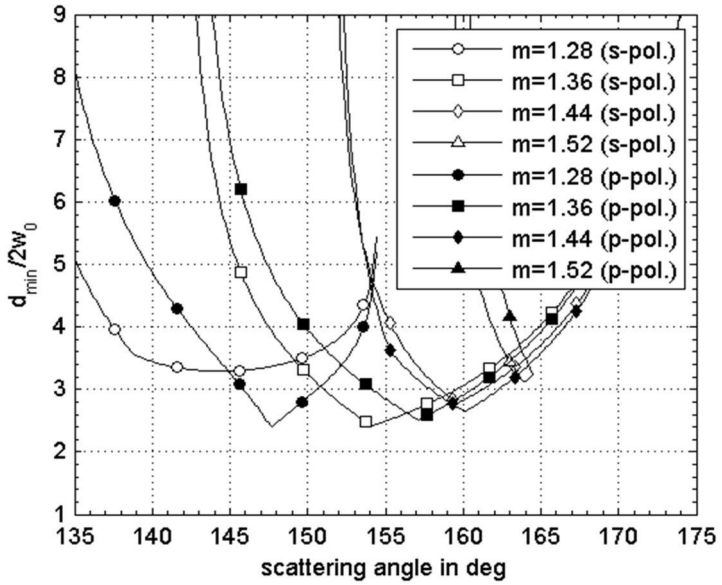

Figure 5: Ratio between the minimal particle size which can be properly detected and the beam width, as a function of scattering angle, computed for different relative refractive indexes and polarization states.

In Figure 6 the optimal scattering angle as a function of refractive index for different polarization states is illustrated. According to this calculation, the optimal scattering angles all lie in near backscatter, which is also a desirable configuration for use in measuring sprays. Moreover, the small angles between the detectors and light source allow compact measurement devices to be desired.

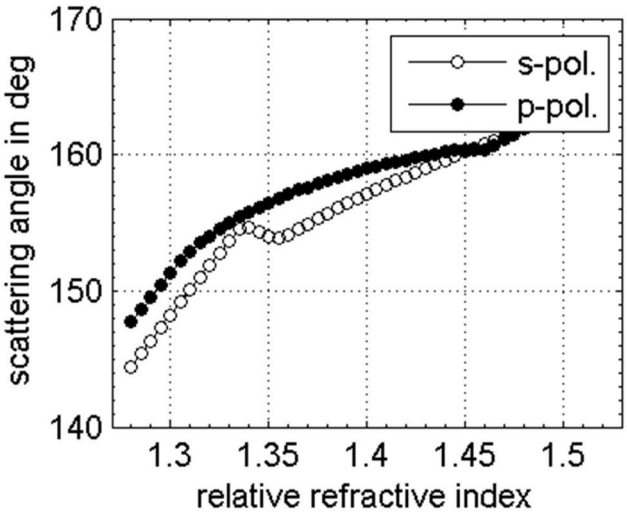

Figure 6: The optimal scattering angle for the best time resolution of the time-shift signal, as a function of relative refractive index calculated for different polarization states.

In Figure 7 two typical time-shift signals are illustrated. The signal depicted on the left has three recognizable peaks, comprising signals from reflection and two modes of second-order refraction; this signal can be easily processed. The second signal, depicted in the right diagram, exhibits a strong overlap of the different signal peaks because the particle/beam ratio is too low; this signal cannot be successfully processed.

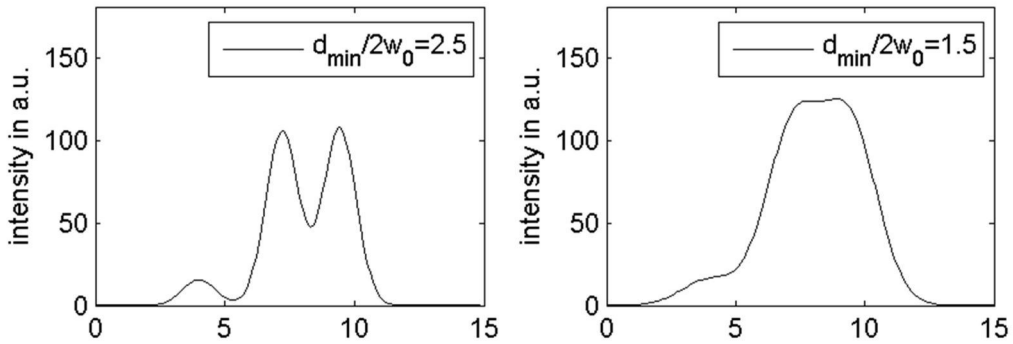

Figure 7: Time-shift signal for d=90µm, v=10m/s, m=1.36, sca=154deg and 2w(left)=36µm, 2w(right)=60µm. The strongest two peaks correspond to second-order refraction and the lower peak corresponds to reflection.

4. Signal Validation

For spray characterization the time-shift technique can only be applied if the detected time-shift signal originates from single, near spherical particles. However, for high density sprays more than one particle could be illuminated at the same time. This results in overlapping signals, which lead to errors in the analysis, as do signals coming from strongly non-spherical particles. Therefore a validation at the signal processing stage is required before calculation of particle size, velocity and refractive index, in order to reject incorrect signals. In this section two such validation criteria are introduced and will be referred to as the 'beta' and 'gamma' conditions; both of these criteria can be derived using geometric optics and are valid only for transparent particles, i.e. particles in which scattering modes of second-order refraction are used in the time-shift technique.

In backscatter, where the reflection (p=0) and the two modes of second-order refraction (p=2.1 and p=2.2) exist, the signal from one detector provides the necessary number of linearly independent

time separations for signal validation. The validation used is expressed as a ratio between time separations between the signal peak arising from reflection and from the two modes of second-order refraction. This validation ratio is called the 'gamma' ratio. From time separations calculated by employing a ray tracing method the 'gamma' ratio is given by

$$\frac{\Delta t_{02}}{\Delta t_{01}} = \frac{\frac{d/2}{v}\left(\cos\left(\frac{\theta_s}{2}\right)+\sin\left(\theta_i^{p=2.2}(\theta_s,m)\right)\right)}{\frac{d/2}{v}\left(\cos\left(\frac{\theta_s}{2}\right)+\sin\left(\theta_i^{p=2.1}(\theta_s,m)\right)\right)} = \frac{\left(\cos\left(\frac{\theta_s}{2}\right)+\sin\left(\theta_i^{p=2.2}(\theta_s,m)\right)\right)}{\left(\cos\left(\frac{\theta_s}{2}\right)+\sin\left(\theta_i^{p=2.1}(\theta_s,m)\right)\right)} := \gamma(\theta_s,m) \quad (14)$$

Consequently the gamma ratio is constant for a given refractive index and a given scattering angle. The graphical representation of Eq. (14) presented in Figure 8 shows values of gamma as a function of scattering angle and relative refractive index. The value of the gamma ratio can therefore be used as a validation of processed signals, if the relative refractive index is known beforehand. This validation helps eliminate errors arising when several particles are simultaneously in the measurement volume or if the time-shift signal arises from a highly non-spherical particle.

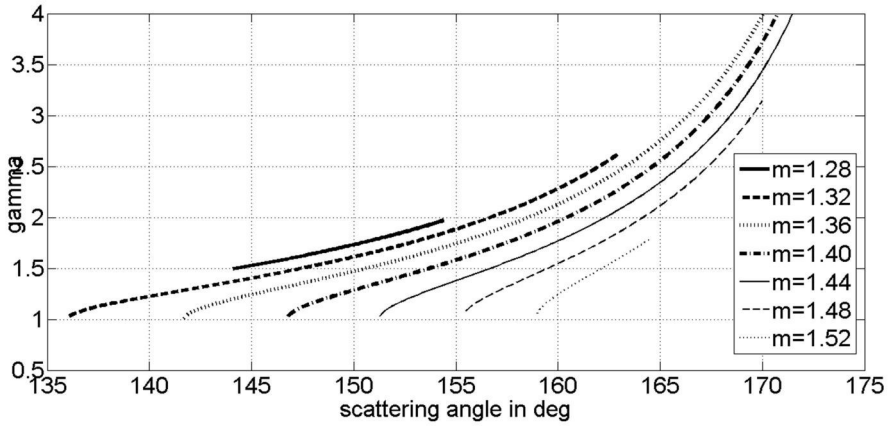

Figure 8: Gamma ratio as a function of scattering angle for different relative refractive indexes.

However, the 'gamma' condition is also applicable to distinguish signals coming from particles with differing refractive indexes. For drying or mixing processes, where the spray consists of two or more distinct components exhibiting different evaporation rates and refractive indexes, it is possible to recognize the respective refractive index of each particle, if sphericity is assumed and if the spray density is not so high, that multiple particle signals can be expected.
Even when the refractive index is unknown, this validation principle can be extended if optical configurations of the time-shift technique with two detectors and one light source are used. In this case, two signals are available. While the correct value of the gamma ratio is not known, it is clear that the gamma ratio must be the same for the signal from each detector and this is then a check on the sphericity of the particle. This condition can be expressed simply as:

$$\gamma^{Detector1}(m,\theta_S) = \gamma^{Detector2}(m,\theta_S) \quad (15)$$

If this condition is fulfilled, then the relative refractive index can be determined from the measured value of the gamma ratio.
If two detectors are used, an additional validation criterion can be formulated, to be called the 'beta'

ratio, which is similar to the 'gamma' ratio but uses time separations between peaks of different signals. This ratio is expressed as:

$$\frac{\Delta t_{22}}{\Delta t_{11}} = \frac{\frac{d/2}{v}\left(2\sin\left(\theta_i^{p=2.2}(\theta_s, m)\right)\right)}{\frac{d/2}{v}\left(2\sin\left(\theta_i^{p=2.1}(\theta_s, m)\right)\right)} = \frac{\sin\left(\theta_i^{p=2.2}(\theta_s, m)\right)}{\sin\left(\theta_i^{p=2.1}(\theta_s, m)\right)} := \beta(\theta_s, m) \tag{16}$$

which, in this form, also assumes that the detectors are placed symmetric about the light source. This symmetry condition is not mandatory, but simplifies the expression somewhat.
The advantage of using the beta ratio is that only the signal peaks arising from second-order refraction are necessary, which often display significantly higher intensity than the reflective peaks, especially in backscatter. Hence lower gain detectors can be used and useable signals can still be obtained even under extenuating measurement conditions, for instance, when high obscuration is present, attenuating the scattered light intensity. Eq. (16) is shown graphically in Fig. 9.

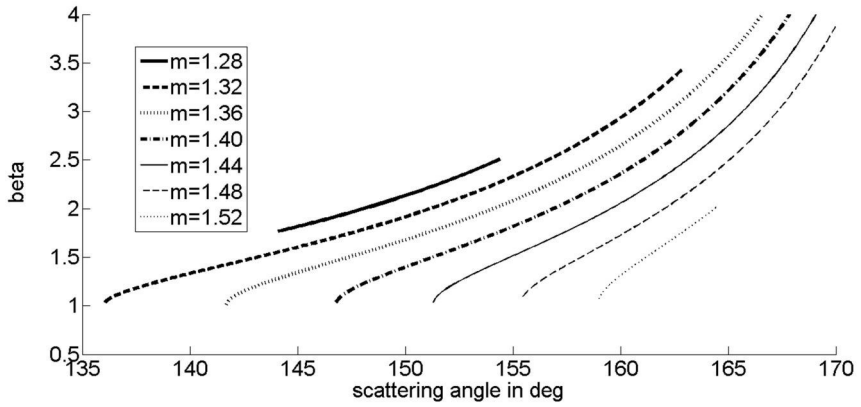

Figure 9: Beta ratio as a function of scattering angle and relative refractive indexes

Another more practical reason for employing the gamma and beta ratios is that the incident angles of second-order refraction modes can be found experimentally. If the detectors or light sources are located symmetrically, the incident angles will be computed by

$$\sin(\theta_i^{p=21}) = \cos\left(\frac{\theta_S}{2}\right)\left(\frac{\gamma - 1}{\beta - \gamma}\right) \tag{17}$$

and

$$\sin(\theta_i^{p=22}) = \cos\left(\frac{\theta_S}{2}\right)\left(\beta\frac{\gamma - 1}{\beta - \gamma}\right) \tag{18}$$

Once these angles are known, the relative refractive index can be calculated by using the following relation, derived using ray tracing:

$$m = \frac{\sin(\theta_i^{p=22})}{\sin\left(\frac{\pi}{4} - \frac{\theta_S}{4} + \frac{\theta_i^{p=22}}{2}\right)} = \frac{\sin(\theta_i^{p=21})}{\sin\left(\frac{\pi}{4} - \frac{\theta_S}{4} + \frac{\theta_i^{p=21}}{2}\right)} \tag{19}$$

Using both the gamma and beta ratios it is therefore possible to not only validate signals but also to determine the relative refractive index. Such information is particularly useful when measuring in spray mixing systems.

5. Measurement Results

One pre-requisite of the time-shift technique is that the illuminating sheet in the measurement volume to be of the same size or smaller than the smallest particle to be measured; hence good focusing characteristics of the illuminating beam are essential for measurements in typical industrial sprays. The laser sheet created in the experimental setup presented in this study has a beam waist of 38µm at a working distance of 200mm; hence only time-shift signals arising from particles larger than about 100µm is possible. In order to test the reliability of the measurement technique falling glass beads with a narrow particle distribution around 250µm were used. The particle size distribution was measured additionally by direct imaging for comparison. These transparent glass particles have an approximately spherical shape, as can be seen in Figure 10. The glass particles were measured in free fall, and the distance between the nozzle exit and the measurement volume was varied between 100mm and 600mm.

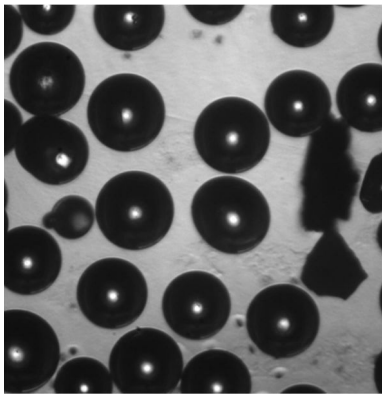

Figure 10: Image of glass particles.

The particle size distribution measured by the time-shift technique is depicted in Figure 11, where measurements performed at different distances from the nozzle (h) are shown. The comparison with the size distribution obtained from direct imaging is very good.

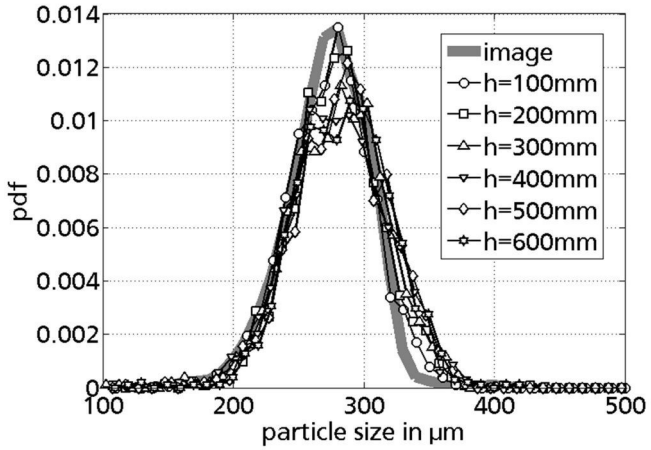

Figure 11: Particle size distribution measured by direct imaging (gray line) and by the time-shift technique.

The particle velocity distributions corresponding to the particle size distributions depicted in Figure 11 are illustrated in Figure 12, where it can be seen that the velocity increases with distance from the exit nozzle (*h*); furthermore the velocity distribution becomes broader. This behavior is consistent with expectations when particles fall into quiescent air.

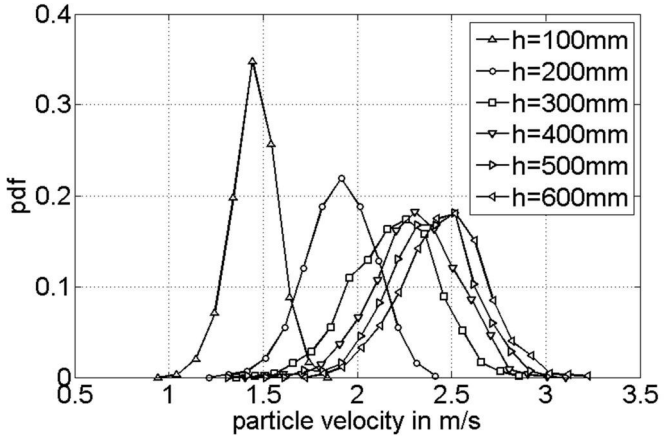

Figure 12: Particle velocity distribution measured by the time-shift technique.

The same experimental setup (Figure 2) was used to measure the refractive index of different spray: water, water/glycerin mixtures and ethanol, using the gamma and beta ratios. The experimental results are illustrated in Figure 13. These results indicate also the approximate resolution of the measured relative refractive index, being about 0.01. Although not high, this resolution is sufficient for some applications in which different materials must be distinguished. The main limiting factor of this resolution is given by peak detection algorithm used for measuring of the time position of individual peaks in a time-shift signal. Any stochastic scatter of this value enters directly into the gamma and/or beta ratio; hence also into the computed relative refractive index. This algorithm is fast but it cannot determine the time position of a peak with sufficient precision, leading to a broadening of the measured relative refractive index distribution illustrated in Figure 13. This limitation can be partly overcome, if instead of peak detection a Gaussian fit to the time-shift signal is used to determine the time position of the peaks. This method is computational more demanding and prohibits real-time processing with the present hardware.

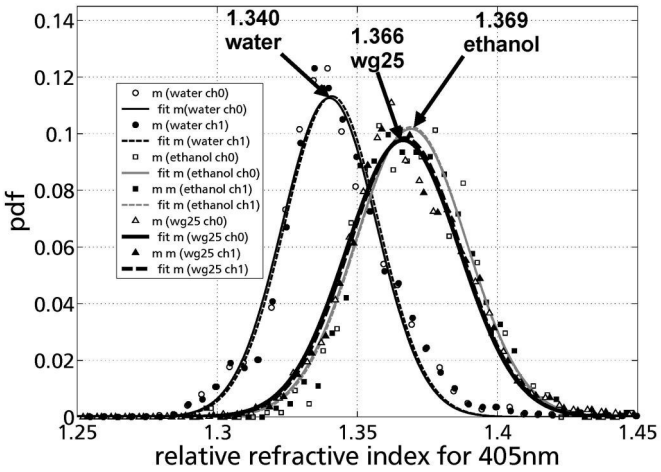

Figure 13: Relative refractive index distribution for water, water/glycerine mixture with 25% concentration (wg25) and ethanol measured by time-shift technique.

6. Conclusion

The time-shift technique presented in this work is suitable for particle velocity and size determination and, in certain configurations and for certain applications also the relative refractive index can be estimated. The new validation principles, applicable for transparent particles, improve the reliability of the measurement technique. Limitations of the technique with respect to scattering angle and relative refractive index have been presented. Moreover the minimal measurable particle size has been expressed as a function of the illumination beam width. In future work the laser sheet thickness should be reduced while maintaining the working distance

7. References

[1] Tropea C 2011 Optical particle characterization in flows. *Ann Rev Fluid Mech*. **43**:399–426

[2] Albrecht H-E, Borys M, Damaschke N, Tropea C 2003 **Laser Doppler and Phase Doppler Measurement Techniques**. Heidelberg: Springer-Verlag

[3] van Beeck JPAJ, Riethmuller ML 1995 Nonintrusive measurements of temperature and size of single falling raindrops. *App. Opt.* **34**, 1633-1639

[4] Semidetnov N 1985 Investigation of laser Doppler anemometer as instrumentation for two-phase flow measurements. PhD Diss. Leningrad Inst. Precis. Mech. Optics, Dept. Opto-Electron. Instrum.

[5] Damaschke N, Nobach N, Semidetnov N, Tropea C 2002 Optical particle sizing in backscatter. *Appl Opt.* **41**:5713-5727

[6] Hess CF, Wood CP 1994 The pulse displacement technique: a single particle counter with a size range larger than 1000:1. *Part Part Syst Charact*. **11**:107–113

[7] Lin SM, Waterman DR, Lettington AH. 2000 Measurement of droplet velocity, size and refractive index using the pulse displacement technique. *Meas Sci Technol*. **11**:L1–4

[8] Debye P. 1909 Der Lichtdruck auf Kugeln von beliebigem Material. *Ann Phys.* **30**:57-136

[9] Mie G. 1908 Beiträge zur Optik trüber Medien, speziell kolloidaler Metallösungen. *Ann Phys.* **25**:377–445

[10] Glantschnig WJ, Chen S-H 1981 Light scattering from water droplets in the geometrical optics approximation. *Appl Opt.* **20**: 2499-2509